Time-Varying Flow Investigation of Synthetic Jet Effects on a Separating Boundary Layer

FRANCESCA SATTA, DANIELE SIMONI, MARINA UBALDI, PIETRO ZUNINO

Department of Fluid Machines, Energy Systems, and Transportation
University of Genova
Via Montallegro 1, I-16145
Genova, ITALY
francesca.satta@unige.it, daniele.simoni@unige.it, marina.ubaldi@unige.it, pietro.zunino@unige.it

FRANCESCO BERTINI

Avio R&D
Via I Maggio, 99, I-10040
Rivalta (TO), Italy
francesco.bertini@aviogroup.com

Abstract: - This paper is focused on the investigation of the interaction between a synthetic jet and the boundary layer which develops over a flat plate subjected to an adverse pressure gradient typical of a high-lift low-pressure turbine profile. Two different Reynolds numbers of the main flow, Re = 200000 and Re = 70000, typical of the low-pressure turbine operating conditions during the take-off/landing and cruise phases, respectively, have been investigated. Wall static pressure distributions along the plate showed the different effects induced by the jet on the boundary layer separation with the jet Strouhal numbers investigated. The device capability of suppressing the large laminar separation bubble which occurs for the uncontrolled condition has been more in depth investigated by means of hot-wire time-mean and ensemble averaged measurements. The phase-locked ensemble averaging technique, synchronized with the synthetic jet frequency, has been employed to distinguish the effects induced by the jet during the blowing and the suction phases. The active device has been proved to be able to control the laminar separation bubble induced by a strong adverse pressure gradient, also at the low Reynolds number condition tested. The ensemble averaged measurements showed that a larger contribution to the reduction of the boundary layer velocity defect is obtained during the suction phase of the jet.

Key-Words: - boundary layer control, separated boundary layer, low-pressure turbines, synthetic jet, phase-locked measurements, hot-wire anemometry.

1 Introduction

Due to the low Reynolds number observed in the low-pressure turbines environment, the boundary layers developing along the profile suction side are mostly laminar, then transitional over a significant length. Therefore, the flow on these profiles may be affected by the occurrence of separations, especially when high-lift profiles operating at low Reynolds number conditions are considered [1-4]. The problem of separation may be attenuated by the beneficial effects induced by upstream wake periodic fluctuations which impinge on the boundary layer, as discussed in several works reported in literature (e. g. [5-8]). However, when this wake-boundary layer interaction is not sufficient to sensibly reduce the separation, the only means for overcoming the occurrence of separation is the exploitation of boundary layer control [9-11].

In spite of their higher complexity and energy requirements, active control devices have a peculiar advantage as compared with passive ones: they can be turned on when necessary and turned off when not necessary and detrimental for losses. This feature makes them attractive for future aero-engine applications.

The paper provides an experimental investigation of the interaction between a synthetic jet (described in [12]) and the boundary layer which

develops along a flat plate installed in a double contoured test section. The contoured walls have been designed to create an adverse pressure gradient typical of an Ultra-High-Lift turbine profile.

Hot-wire investigations have been performed to analyse the jet effects on the transition and separation processes taking place within the boundary layer.

In particular, phase-locked diagrams of the ensemble-averaged velocity and turbulence intensity have been provided to recognize the separate effects of the blowing and the suction phases of the jet.

The work reported in this paper has been carried out within a research collaboration between University of Genova and Avio, in the frame of the European project TATMo (Turbulence And Transition Modeling for Special Turbomachinery Applications).

2 Experimental apparatus and measurement techniques

Measurements have been performed in an open loop wind tunnel installed in the Aerodynamics and Turbomachinery Laboratory of the University of Genova.

The test section (Fig. 1) is constituted by a flat plate installed between two contoured walls that produce the desired adverse pressure gradient, typical of an Ultra-High-Lift turbine profile. The flat plate is 200 mm long and 300 mm wide.

Figure 1: Double contoured test section.

In order to provide the zero net mass flow rate condition for the synthetic jet, a mechanical piston generating an intermittent mass flow rate has been adopted. The piston has been connected to a cavity obtained within the upper side of the flat plate to control the boundary layer separation provoked by the adverse pressure gradient. The synthetic jet system (Fig. 2) is more extensively described in [12]. The axis of the jet is located at a distance equal to 30% of the plate length from the leading edge, just behind the velocity peak and upstream of the position where separation begins in the uncontrolled case.

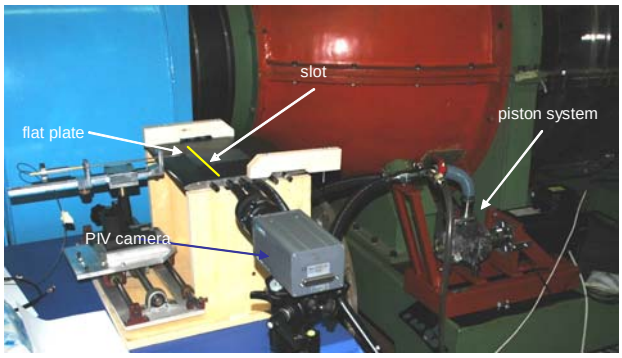

Figure 2: Synthetic jet generation system.

The flat plate has been instrumented at midspan, along its rear part (downstream of the velocity peak), with a total of 25 pressure taps connected to a Scanivalve. The pressures have been measured by means of high-sensitivity high accuracy low range SETRA differential transducers. The instrument accuracy is better than ±0.075% of the transducer full-scale range (±620 Pa).

Hot-wire measurements have been performed at x/L = 0.45, inside the boundary layer laminar separation bubble, which takes place when control is not applied.

Boundary layer velocity distributions have been investigated with 31 points along the line normal to the wall, with smaller spacing close to the wall. A computer controlled traversing mechanism with a minimum linear translation step of 8μm has been employed to allow high movement precision and spatial resolution. The boundary layer development has been investigated within a Reynolds numbers range of 70000-200000. Measurements have been carried out for both uncontrolled and controlled boundary layers (without and with the synthetic jet installed).

For the controlled case, four different jet Strohual numbers, and consequently different velocity ratios and momentum coefficients, have been tested in order to search the most suitable jet condition for the different Reynolds numbers. The main aerodynamic parameters of the jet for the different jet conditions investigated are reported in Table 1.

Even though the flow direction in a separation bubble cannot be determined with a single sensor hot-wire, an estimate of the velocity magnitude can be obtained and it has been found to be very low and nearly constant within the bubbles investigated in the present study.

Table 1: Synthetic jet aerodynamic parameters.

Condition	*r*	St
f_1	0.235	0.125
f_2	0.314	0.167
f_3	0.471	0.25
f_4	0.942	0.5

Since the experimental velocity records contain both periodic unsteadiness, associated with the synthetic jet frequency, and other velocity fluctuations associated with turbulence and unsteadiness not at the jet frequency, the ensemble averaging technique has been employed to distinguish these two effects. The reference signal has been derived from the encoder applied to the synthetic jet system shaft. Three contiguous jet periods have been measured, collecting 100 data for each period, with a consequent dimension of each sampled record of 300 data. Moreover, 250 piston revolutions have been considered for the ensemble average in order to obtain a satisfactory statistical accuracy.

3 Results and discussion

3.1 Pressure distributions

Blade loadings measured in the rear part of the plate under uncontrolled and controlled conditions are plotted in terms of the static pressure coefficient (C_p) in Figs. 3 and 4, for Re=200000 and Re=70000, respectively. The jet conditions tested for the controlled cases are those reported in Table 1.

At Re=200000, in the case without control (baseline flat plate), the occurrence of boundary layer laminar separation is revealed by the plateau in the C_p distribution. Boundary layer separation begins at x/L equal to about 0.39, and the reattachment is completed at x/L = 0.49.

The small laminar separation bubble which characterizes the uncontrolled condition seems to be completely suppressed by the jet even with the smallest Strouhal number (f_1: St = 0.125). The separation suppression generates a load increase in the front part of the flat plate. For this Reynolds number, an increase of the jet frequency does not introduce further benefits, since the separation bubble occurring in the uncontrolled case is small. Thus, the higher energy expenditure requested to produce the jet with a Strouhal number larger than 0.125 is wasted.

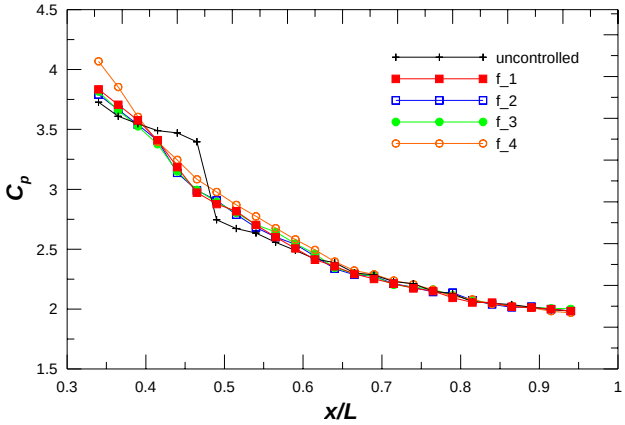

Figure 3: Pressure coefficient distributions at Re=200000.

As the Reynolds number decreases (Re = 70000) and not any control device is applied, the pressure coefficient plateau becomes much more extended (Fig. 4), indicating that the laminar separation bubble affects a larger surface portion. In fact, the boundary layer separates at about the same position observed for Re = 200000, but reattaches sensibly downstream, at x/L= 0.69.

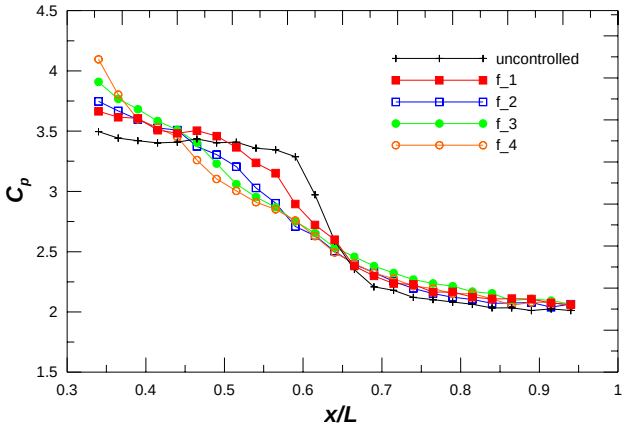

Figure 4: Pressure coefficient distributions at Re=70000.

For this Reynolds number, the differences between the jet conditions tested become appreciable. In this case, in fact, due to the very

long laminar separation bubble occurring when the boundary layer is not controlled, the jet with St = 0.125 (f_1) introduces only a very small benefit in terms of separation reduction. The laminar separation seems to be completely suppressed only for Strouhal numbers higher than 0.25. This feature suggests that the momentum introduced in the boundary layer by the synthetic jet to prevent the laminar separation should be enhanced when the Reynolds number decreases, because of the separation bubble enlargement occurring.

3.2 Hot-wire results

In order to better understand the effects induced by the jet on the boundary layer laminar separation, in Figs. 5-8 the time-mean velocity and turbulence intensity profiles measured at *x/L*=0.45 for two different jet conditions (f_1 and f_3) are reported, for Re = 200000 and Re = 70000. At the highest Reynolds number (Figs. 5 and 6), in the uncontrolled case the separation bubble extends up to *y/L* =0.004.

For this Reynolds number condition, the jet is able to completely suppress the laminar separation for both Strouhal numbers tested, as suggested by the shape of the velocity distributions close to the wall (Fig. 5). The comparison of the two jet conditions shows that the jet with the smaller Strouhal number (*St*=0.125) is able to provide a fuller boundary layer profile, as compared with the higher Strouhal number case. The turbulence intensity distributions (Fig. 6) show higher values occurring in the two controlled cases as compared with the uncontrolled one. This increase is due to the large scale coherent structures introduced in the boundary layer by the jet during the blowing phase (these structures have been observed for example in [12] and [13]), as well as to the mean velocity low frequency oscillations associated with the jet period. Moreover, the turbulence intensity assumes larger values at the largest Strouhal number, probably due to a stronger interaction between the jet and the main flow provoked by the larger amplitude of the jet velocity oscillations.

At Re = 70000, the separation bubble becomes more extended, and at *x/L*=0.45 the boundary layer is completely separated as revealed by both mean velocity (Fig. 7) and turbulence intensity (Fig. 8) distributions. In particular, this latter quantity shows a peak occurring in correspondence of the separated shear layer (just above the stagnant fluid region where strong shear effects are present) as typically observed in literature for laminar separated boundary layers [14-17].

For this Reynolds number, due to the thicker separation bubble which characterizes the uncontrolled case, the jet with St = 0.125 does not seem to be able to completely suppress the separation, as suggested by the local inflection in the velocity profile (red curve in Fig. 7). This observation is consistent with the pressure coefficient distributions comparison. Thus, at Re = 70000, a higher frequency jet is required to sensibly reduce the separation, as revealed by the fuller velocity profile obtained with St = 0.25.

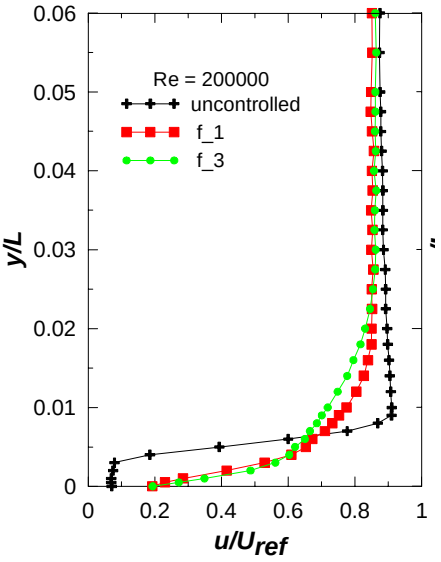

Figure 5: Velocity distributions at x/L=0.45 and Re=200000.

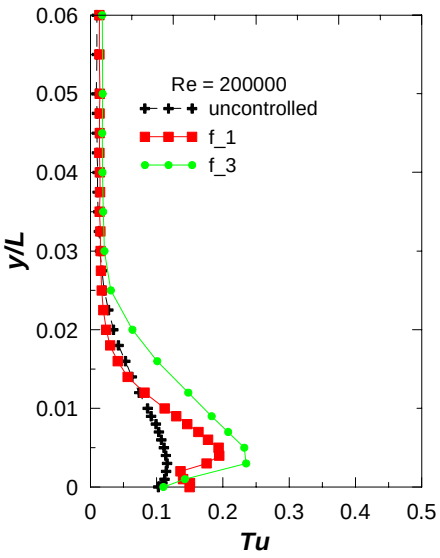

Figure 6: Turbulence intensity distributions at x/L=0.45 and Re=200000.

The turbulence intensity distributions show that, unlike what observed for the largest Reynolds number, at Re = 70000 smaller turbulence intensity

values occur with the largest Strouhal number as compared with the lowest one. It confirms that at Re = 70000 the larger Strouhal number jet better interacts with the main flow, not only because provides a fuller velocity profile, but also because provokes a smaller increase of the velocity fluctuations.

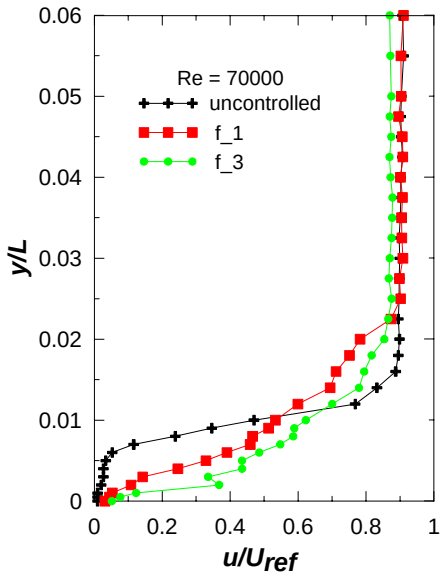

Figure 7: Velocity and turbulence intensity distributions at x/L=0.45 and Re=70000.

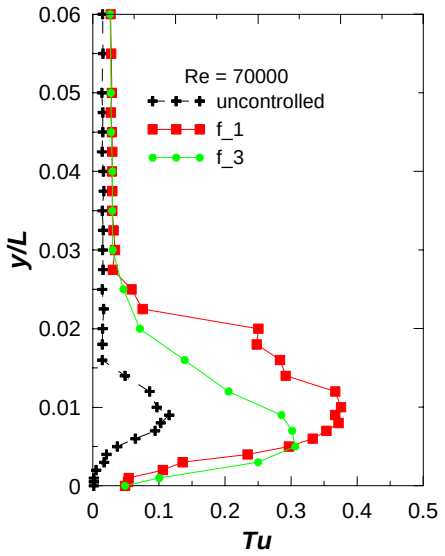

Figure 8: Turbulence intensity distributions at x/L=0.45 and Re=70000.

To distinguish the different working phases effects (the suction and the blowing ones) during the interaction process between the jet and the boundary layer, phase-locked measurements have been performed. The results are shown for the same axial position given for the time-mean measurements (x/L=0.45).

In Figs. 9-12, the phase-locked velocity profiles measured at the middle of the blowing and the suction phases (t/T = 0.0 and t/T = 0.5, respectively) for the two Strouhal numbers are compared with the time-mean profiles measured for Re = 200000 and Re = 70000.

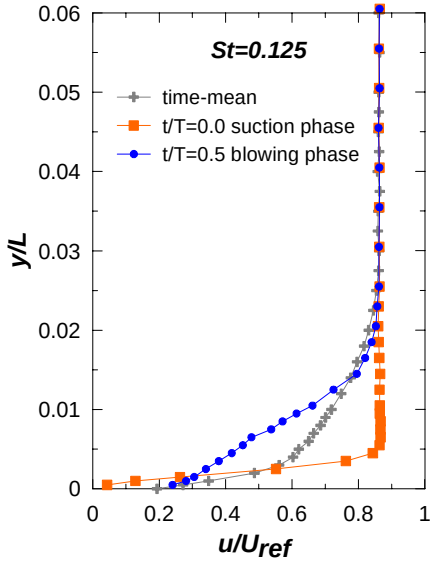

Figure 9: Velocity profiles comparison at x/L=0.45, for Re=200000 and St=0.125.

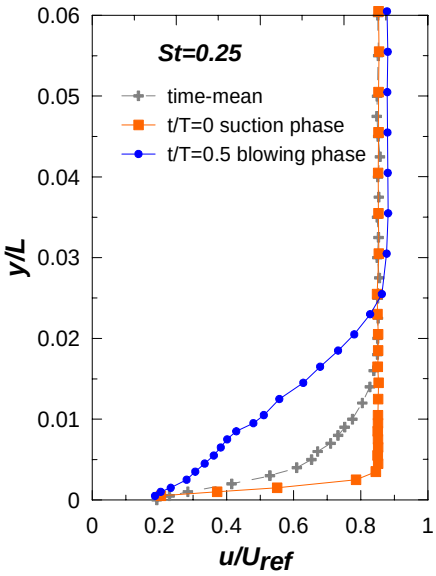

Figure 10: Velocity profiles comparison at x/L=0.45, for Re=200000 and St=0.25.

In correspondence of t/T = 0.0 (suction phase) for all the Reynolds and Strouhal numbers investigated, the boundary layer is thinner. During the blowing phase (t/T = 0.5) the velocity defect is much larger and affects a more extended distance

from the wall. Overall, as already shown, the synthetic jet effect is positive in terms of averaged velocity profiles.

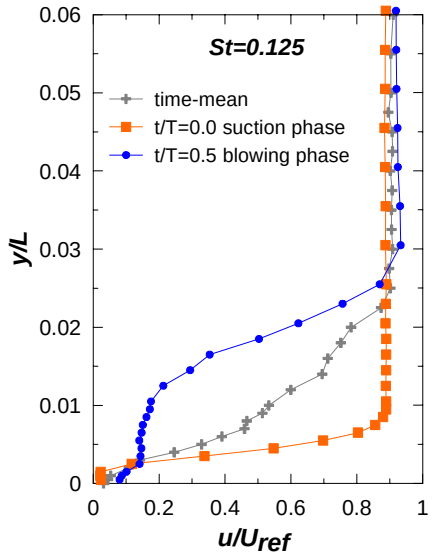

Figure 11: Velocity profiles comparison at x/L=0.45, for Re=70000 and St=0.125.

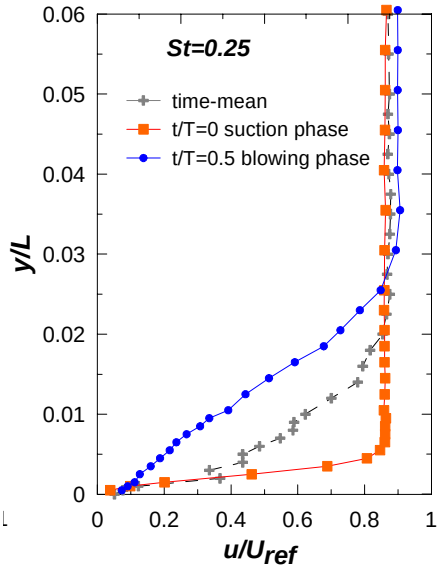

Figure 12: Velocity profiles comparison at x/L=0.45, for Re=70000 and St=0.25.

To better understand the jet-boundary layer interaction mechanisms during the whole jet cycle, phase-locked measurements results have been reported also in time-space diagrams.

In Figs. 13 and 14, the ensemble-averaged velocity and turbulence intensity colour plots are reported for St = 0.125 and *St*=0.25 respectively, at *Re* = 200000.

The jet blowing phase can be identified by the high turbulence intensity signature, observable close to the wall in the range $0.25<t/T<0.75$, and provoked by the large scale coherent structures introduced by the jet. In correspondence of this non-dimensional time interval, the ensemble-averaged velocity colour plot shows a strong velocity defect, significantly extended in the direction normal to the wall at both the two jet frequencies. That suggests that during the blowing phase a strong interaction between the jet and the boundary layer takes place, provoking a deceleration in the main flow and a consequent blockage effect. This effect counteracts the beneficial effect introduced by the mixing increase associated with the large vortical structures.

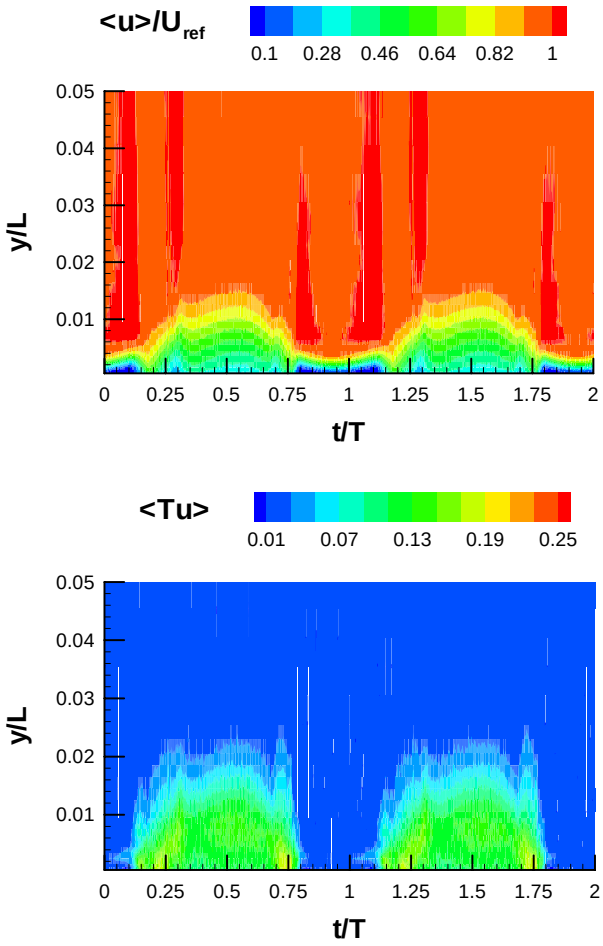

Figure 13: Velocity and turbulence intensity colour plots at x/L=0.45: Re=200000 and St=0.125.

During the suction phase of the jet ($0.75<t/T<1.25$), the separated boundary layer tends to be removed within the cavity. Thus, the boundary layer appears to be in a better condition as compared with the blowing phase. In fact, during the jet ingestion phase, the high momentum fluid particles coming from the outer part of the boundary layer are forced to move towards the wall giving a contribution to the boundary layer time-mean

laminar separation prevention. Moreover, the turbulence intensity colour plots for both the Strouhal number conditions reveal that during the ingestion phase the boundary layer is in a laminar condition, as demonstrated by the absence of velocity fluctuations within the boundary layer.

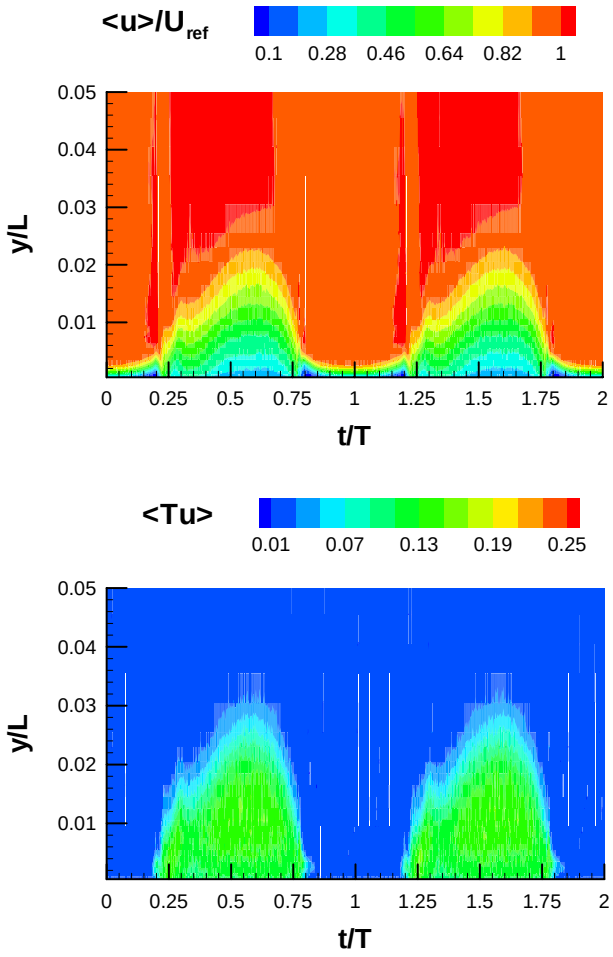

Figure 14: Velocity and turbulence intensity colour plots at x/L=0.45: Re=200000 and St=0.25.

At this Reynolds number condition, the low velocity area which characterizes the blowing phase becomes larger as the jet Strouhal number increases. Similarly, also the turbulence intensity colour plots show a larger area affected by high velocity fluctuations occurring at the higher Strouhal number condition. Thus, both the ensemble-averaged velocity and turbulence intensity colour plots confirm that at Re = 200000 is inconvenient to adopt a Strouhal number for the jet larger than 0.125.

Also at Re = 70000, the ingestion phase of the jet seems to introduce greater benefits as compared with the ejection phase, like demonstrated by the ensemble-averaged velocity colour plots reported in Figs. 15 and 16 for St = 0.125 and 0.25, respectively.

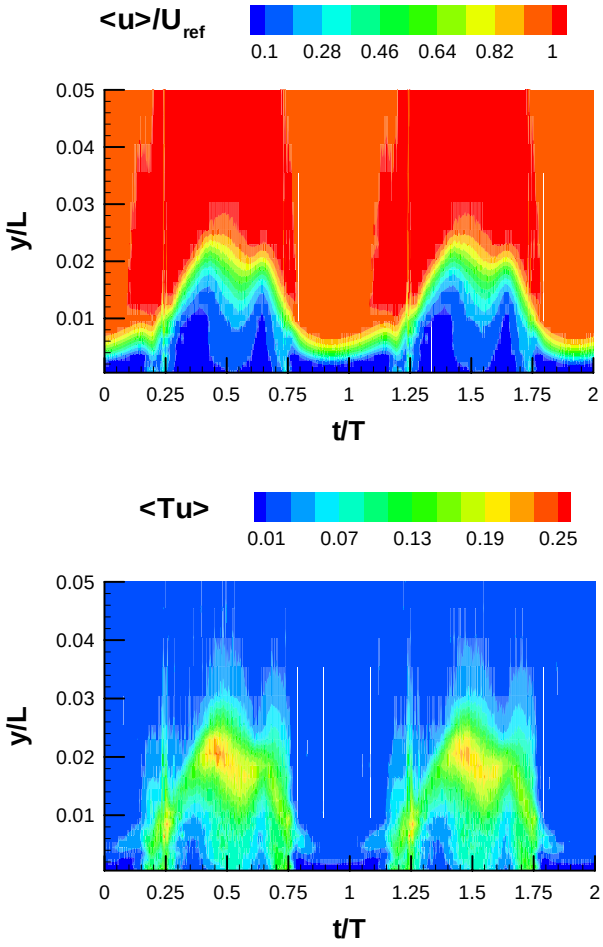

Figure 15: Velocity and turbulence intensity colour plots at x/L=0.45: Re=70000 and St=0.125.

The ensemble averaged velocity distributions show that the smaller velocity defect achieved for the larger Strouhal number jet, revealed by the time-mean measurements, originates from both the blowing and the suction phases of the jet. In fact, the velocity defect close to the wall during the blowing phase becomes smaller as the Strouhal number increases. Furthermore, the capability of the jet during the suction phase of reducing the separation extension is sensibly increased with the larger Strouhal number (Fig. 15).

Also the ensemble averaged turbulence intensity colour plots confirm, as previously noticed in the time-mean distributions, that at this Reynolds number the smaller velocity fluctuations area is produced when the larger Strouhal number is adopted.

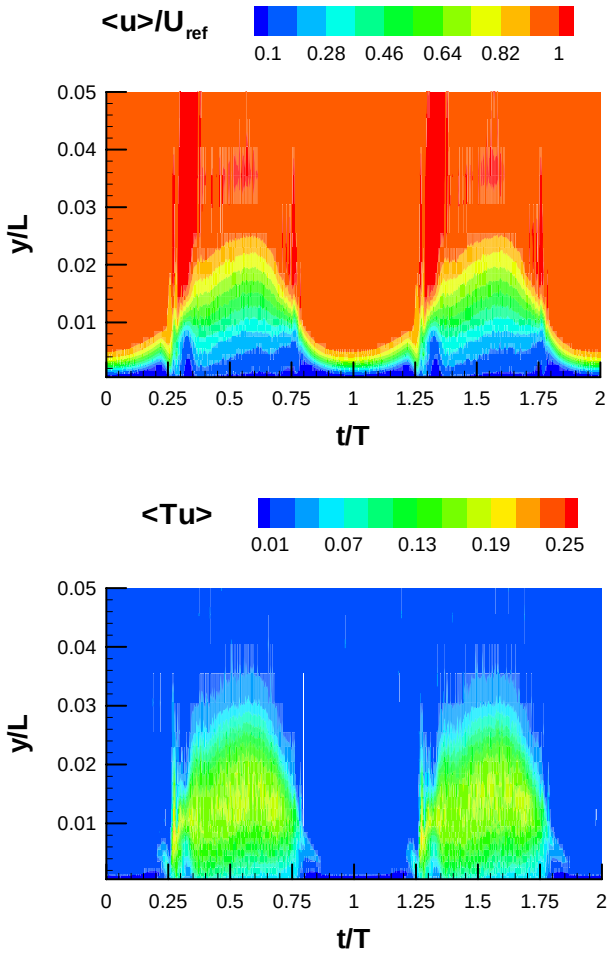

Figure 16: Velocity and turbulence intensity colour plots at x/L=0.45: Re=70000 and St=0.25.

4 Conclusions

The present work has been focused on the study of the interaction between a synthetic jet and the boundary layer which develops over a flat plate with an adverse pressure gradient typical of a high-lift low-pressure turbine profile. Two different main flow Reynolds numbers, typical of the low-pressure turbine operating conditions, as well as different synthetic jet Strouhal numbers have been investigated.

Hot-wire anemometer and static pressure taps have been adopted to survey the boundary layer which develops over the flat plate, for both the uncontrolled and controlled cases (without and with the synthetic jet installed, respectively). Phase-locked measurements have been also carried out by means of the hot-wire anemometer to allow the investigation of the time-dependent velocity profiles and distinguish the two main phases of the jet.

When boundary layer control is not applied, the pressure coefficient distributions revealed the presence of a laminar separation bubble at both the Reynolds number conditions tested. The bubble length and thickness have been found to be sensibly higher at the lower Reynolds number, as revealed by the pressure coefficients as well as by the time-mean velocity and turbulence intensity distributions.

Both static pressure and time-mean velocity measurements showed the synthetic jet capability of reducing the boundary layer laminar separation which occurs for the uncontrolled condition. In particular, at Re = 200000, where a small laminar separation bubble in the uncontrolled case has been found, the jet with the smallest Strouhal number resulted to be sufficient to completely suppress the separation. On the contrary, at Re = 70000, the jet with the highest Strouhal number was requested to suppress the large laminar separation bubble occurring for the uncontrolled condition.

The phase-locked velocity profiles allowed the distinction between the effects induced by the jet during the blowing and the suction phases. A strong interaction between the jet and the boundary layer has been detected during the blowing phase, as shown by the high turbulence intensity region taking place during this phase, provoked by the large scale vortical structures introduced by the jet. The ejected flow induces a strong velocity defect also far away from the wall but allows the reduction of the laminar separation when the appropriate jet Strouhal number is adopted. During the suction phase of the jet, the separated flow is removed within the cavity and the high momentum flow coming from the outer part of the boundary layer is transferred in the region next to the wall, provoking the reduction or even the suppression of the laminar separation bubble. Moreover, the turbulence intensity colour plots for all the Reynolds and Strouhal numbers conditions investigated revealed that during the ingestion phase the boundary layer is in a laminar state, since no velocity fluctuations within the boundary layer have been detected during this phase and the phase-locked boundary layer velocity profile is linear.

The unbeneficial effect associated with the blowing phase for all the conditions investigated points out the necessity of developing and testing an improved synthetic jet system, characterized by a smaller flow rate injected during the blowing phase.

5 Acknowledgements

The authors gratefully acknowledge the financial support of the European Commission as part of the research project TATMo, 'Turbulence And Transition Modeling for Special Turbomachinery Applications'.

Nomenclature

C_p	pressure coefficient $= \frac{p_{t0} - p}{p_{t0} - \overline{p_0}}$
f_{act}	device frequency
L	flat plate length
p	static pressure
p_t	total pressure
r	velocity ratio
Re	flat plate length Reynolds number
St	Strouhal number $St = \frac{f_{act} L}{U_0}$
t	time
T	jet period
Tu	turbulence intensity
u	velocity
U_{ref}	boundary layer edge velocity
x	streamwise direction
y	normal to the wall direction

Subscripts and brackets

0	at the test section inlet
$<>$	ensemble averaged quantity

References:

[1] Mayle, R. E., The Role of Laminar-Turbulent Transition in Gas Turbine Engines, *ASME Journal of Turbomachinery*, Vol. 113, pp. 509-531, 1991.

[2] Denton, J.D., Loss Mechanisms in Turbomachines, *ASME Journal of Turbomachinery*, Vol. 115, 1993, pp. 621-656.

[3] Hatman, A., and Wang, T., A Prediction Model for Separated Flow Transition, *ASME Journal of Turbomachinery*, 121, pp. 594–602, 1999.

[4] Hourmouziadis, J., Aerodynamic Design of Low Pressure Turbines, *AGARD Lecture Series*, 167, 1989.

[5] Halstead, D.E., Wisler, D.C., Okiishi, T., Walker, G.J., Hodson, H.P., and Shin, H.W., Boundary Layer Development in Axial Compressor and Turbines: Part 1 of 4-Composite Picture, *ASME Journal of Turbomachinery*, Vol. 119, pp. 114-127, 1997.

[6] Schröder, Th., Investigation of Blade Row Interaction and Boundary Layer Transition Phenomena in a Multistage Aero Engine Low-Pressure Turbine by Measurements with Hot-Film Probes and Surface-Mounted Hot-Film Gauges, in Boundary Layers in Turbomachines, *VKI Lecture Series*, 1991.

[7] Mailach, R., and Vogeler, K., Aerodynamic Blade Row Interaction in an Axial Compressor – Part I: Unsteady Boundary Layer Development, *ASME Journal of Turbomachinery*, Vol. 126, pp. 35-44, 2004.

[8] Hodson, H. P., and Howell R.J., The Role of Transition in High-Lift Low Pressure Turbines for Aeroengines, *Progress in Aerospace Sciences*, Vol. 41, pp. 419-454, 2005.

[9] Himmel CG, Hodson HP, Effective Passive Flow Control for Ultra-High Lift Low Pressure Turbines, *proceedings of the 8th ETC conference*, 2009.

[10] Gad-el-Hak, M., Flow Control, Passive, Active, and Reactive Flow Management, *Cambridge University Press*, Cambridge, 2000.

[11] Volino, R. J., Separation Control on Low-Pressure Turbine Airfoils Using Synthetic Vortex Generator Jets, *ASME Journal of Turbomachinery*, Vol. 125, pp. 765-777, 2003.

[12] Satta, F., Simoni, D., Ubaldi, M., Zunino, P., Design and Aerodynamic Characterization of a Synthetic Jet for Boundary Layer Control, *proceedings of the 5th WSEAS int. conf. on Applied and Theoretical Mechanics (Mechanics '09)*, 2009.

[13] Hayes-McCoy, D., Jiang, X., Lockerby, D., Analysis of Zero-Net-Mass-Flux Synthetic Jets using DNS, *WSEAS Transactions on Fluid Mechanics*, Vol. 3, pp. 47-55, 2008.

[14] Satta, F., Simoni, D., Ubaldi, M., Zunino, P., Bertini, F., 2009, Incoming Wakes Effects on

the Boundary Layer of a High-Lift Low-Pressure Turbine Profile at Low Reynolds Number, 9th ISAIF Conference, Gyeongju, Korea, 8-11 September 2009.

[15] Lou, W., and Hourmouziadis, J., Separation Bubbles Under Steady and Periodic-Unsteady Main Flow Conditions, *ASME Journal of Turbomachinery*, Vol. 122, pp. 634–643, 2000.

[16] Pauley, L. L., Moin, P., Reynolds, W. C., The Structure of Two-Dimensional Separation, *Journal of Fluid Mechanics*, Vol. 220, pp. 397-411, 1990.

[17] Yang, Z., and Voke, P. R., Large-Eddy Simulation of Bounday-Layer Separation and Transition at a Change of Surface Curvature, *Journal of Fluid Mechanics.*, Vol. 439, pp. 305-333, 2001.